Eur. Phys. J. B **25**, 53–60 (2002)
DOI: 10.1140/e10051-002-0007-9

THE EUROPEAN PHYSICAL JOURNAL B
EDP Sciences

Kink solutions of the classical transverse field Ising chain

A. Johann[a]

Technische Universität München, Zentrum Mathematik, 80290 München, Germany

Received 23 February 2001 and Received in final form 4 October 2001

Abstract. We investigate stationary and travelling wave solutions of the classical one-dimensional transverse field Ising model. Results are given on the existence, shape and stability of kink solutions and periodic solutions. We review recent analytical results (*e.g.*, the proof of existence of a one-parameter family of stationary kink solutions and the proof of existence of travelling wave kink solutions with nonzero velocity $c \neq 0$) and extend them by the use of numerical methods. Small oscillations arising in the tails of travelling kink solutions are investigated numerically. In the end, stability analysis puts some light on pinning effects.

PACS. 05.45.Yv Solitons – 75.10.Hk Classical spin models

1 Introduction

One-dimensional spin systems are of great interest in the analysis of quasi one-dimensional magnetic chains (*cf.* [5]). A lot of work has been done on the analysis of both, quantum and classical models (*e.g.*, the XYZ model and its special cases, the Heisenberg model and the Ising model). Many of these models turn out to be completely integrable. However, this article deals with a non-integrable model system, the classical transverse field Ising chain. Our goal is the investigation of basic types of solutions. While we are unable to give a closed expression for any nontrivial solution, it is still possible to give a proof of existence in many cases. Giving existence proofs for certain types of solutions was the main topic of the previous work [4] by the author. In the present article we investigate those types of solutions numerically in order to obtain further information.

This article is primarily concerned with the analysis of domain wall motion. The domain walls can travell trough the lattice under the influence of an external transverse magnetic field. A single domain wall in a double sided infinitely extended chain will be represented by a kink solution. Easily spoken, this is a solution, interpolating in space between two disjoint ground states. We will give results on the domain of existence, shape, energy and stability of both, stationary and travelling wave kink solutions.

In Section 2 we present the equations of motion and some preliminary results on translationally invariant solutions (*i.e.*, solutions constant in space).

Stationary (*i.e.*, time independent) kink solutions are considered in Section 3. Besides the well known CS and CB solutions (classified by their reflectional symmetry in space; for a precise definition see below) an additional one-parameter family of stationary kink solutions exists for an open set of parameter values. Numerical results on the energy of kink solutions and the Peierls-Nabarro barrier will be given.

Section 4 is concerned with travelling wave solutions. First, we give a short survey on periodic solutions. Possible periods of these solutions can be calculated explicitly. The remainder of this section is concerned with nonstationary kink solutions. Their existence can be proved analytically. We give an asymptotic expression for their shape in the continuum limit. The domain of existence of kink solutions in parameter space will be calculated numerically. Furthermore, numerical results lead to an understanding of oscillations in the tail of travelling kink solutions with nonzero velocity. The energy of the central kink and the energy density of the oscillations in the tail will be calculated, too.

In Section 5 we investigate the stability of the solutions considered above. This is done by spectral methods. One application of stability analysis is a better understanding of pinning effects.

2 Preliminaries

We consider the Hamiltonian

$$H = \lim_{n\to\infty} H(-n, n) \tag{1}$$

with the local Hamiltonian

$$H(a,b) = -2J\left[\sum_{x=a}^{b-1} s_1(x)s_1(x+1) + \lambda \sum_{x=a}^{b} s_3(x)\right]. \tag{2}$$

By $s_i(x)$, $i = 1, 2, 3$ we denote the spin components at the lattice site $x \in \mathbb{Z}$. $\lambda \in \mathbb{R}$ denotes the strength of a transverse magnetic field. Without loss of generality, we can choose the coupling constant $2J \neq 0$ to be positive. The sign of $2J$ can be inverted by a 180° rotation of spins

[a] e-mail: johann@mathematik.tu-muenchen.de

around the 3 axis at every other site (for example at every odd site) and the transition $\lambda \to -\lambda$. In addition, we can choose $2J = 1$ by a time gauge. Furthermore, we restrict our attention to chains of the same spin $s(x) = \sqrt{s_1^2(x) + s_2^2(x) + s_3^2(x)}$ at every lattice site x. We choose the spin $s(x)$ to be equal to 1.

Using the Poisson brackets

$$[s_i(x), s_j(y)] = \delta_{xy} \sum_{k=1}^{3} \varepsilon_{ijk}\ s_k(x) \tag{3}$$

and

$$\dot{s}_i(x,t) = \lim_{n\to\infty} [s_i(x,t), H(-n,n)] \tag{4}$$

we obtain the following equations of motion

$$\begin{aligned}
\dot{s}_1(x,t) &= \lambda s_2(x,t) && (5)\\
\dot{s}_2(x,t) &= -\lambda s_1(x,t) + s_3(x,t)\,(s_1(x-1,t) + s_1(x+1,t))\\
\dot{s}_3(x,t) &= -s_2(x,t)\,(s_1(x-1,t) + s_1(x+1,t))\,.
\end{aligned}$$

The most simple solutions of equation (5) are translationally invariant stationary solutions (*i.e.*, solutions constant in time and space). Using the ansatz $s_i(x,t) = s_i$ together with the normalization condition $s_1^2+s_2^2+s_3^2 = 1$, we obtain the following solutions of this type for (s_1, s_2, s_3)

$$\left(\pm\sqrt{1-\frac{\lambda^2}{4}},\ 0,\ \frac{\lambda}{2}\right) \qquad \text{for } -2 < \lambda < 2 \tag{6}$$

$$(0,\ 0,\ \pm 1) \tag{7}$$

$$(0,\ \cos(\mu),\ \sin(\mu)) \qquad \text{for } \lambda = 0 \text{ and } \mu \in \mathbb{R}. \tag{8}$$

The energy density (*i.e.*, mean energy per lattice site) of this solutions equals $-\left(1+\frac{\lambda^2}{4}\right)$ in the first case, $\mp\lambda$ in the second case, and 0 in the last case. For $|\lambda| \geq 2$, the transverse field dominates the next neighbour interaction. Therefore, the ground state is given by the solution $(0, 0, \mathrm{sgn}(\lambda))$. At the bifurcation points $|\lambda| = 2$ the next neighbour interaction starts dominating and the groundstate pitchforkes into two groundstates (6) and a solution $(0, 0, \mathrm{sgn}(\lambda))$ with higher energy density. In the case $|\lambda| < 2$ of ground state degeneration, kink solutions have been proved to exist. They will interpolate in space between two distinct translationally invariant solutions which have the same energy density.

3 Stationary kink solutions

If we consider stationary (*i.e.*, time independent) solutions of equation (5), we obtain the following set of difference equations for the spin components $s_i(x)$; $i = 1, 2, 3$; $x \in \mathbb{Z}$

$$\begin{aligned}
0 &= \lambda s_2(x) && (9)\\
0 &= -\lambda s_1(x) + s_3(x)\,(s_1(x-1) + s_1(x+1))\\
0 &= -s_2(x)\,(s_1(x-1) + s_1(x+1))
\end{aligned}$$

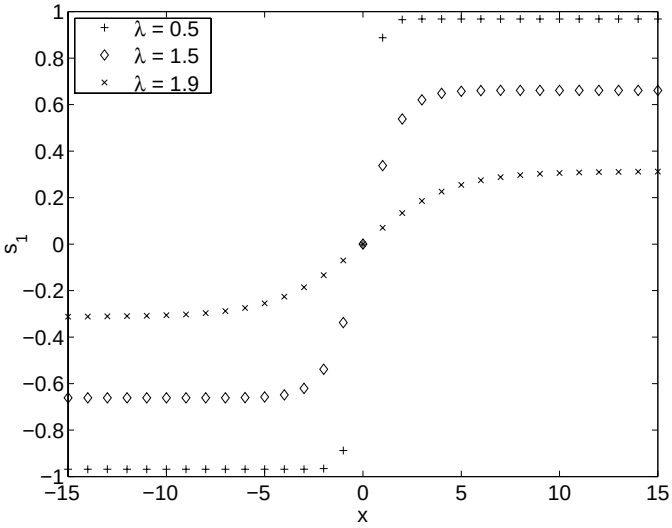

Fig. 1. CS solutions for different values of λ.

together with the normalization condition

$$s_1^2(x) + s_2^2(x) + s_3^2(x) = 1 \tag{10}$$

for each $x \in \mathbb{Z}$. In the case $\lambda \neq 0$, we obtain directly $s_2(x) = 0$ for all x.

If $\lambda = 0$, there are two basic types of kink solutions, namely

$$(s_1(x), s_2(x), s_3(x)) = \begin{cases} (-1,0,0) \text{ for } x < 0 \\ (\mu_1, \mu_2, \mu_3) \text{ for } x = 0 \\ (1,0,0) \text{ for } x > 0 \end{cases} \tag{11}$$

$$(s_1(x), s_2(x), s_3(x)) = (0, \cos(\nu(x)), \sin(\nu(x))) \tag{12}$$

with $\mu_i \in \mathbb{R}$, $\mu_1^2+\mu_2^2+\mu_3^2 = 1$ and a real valued function $\nu\colon \mathbb{Z} \to \mathbb{R}/2\pi$ with $\lim_{x\to-\infty} \nu(x) \neq \lim_{x\to\infty} \nu(x)$. Solution (12) is an exceptional case for vanishing field $\lambda = 0$. Two special cases of solution (11) will be important in the following. They are classified by their reflectional symmetry in the s_1 component. In the case $\mu_1 = 0$, solution (11) is symmetric under spin inversion and spatial reflection with respect to a lattice site. Therefore, it is called *central spin* (CS). In the case $\mu_1 = \pm 1$, solution (11) is symmetric under spin inversion and spatial reflection with respect to the center between two neighboured lattice sites. It is called *central bond* (CB).

CS and CB solutions are well known in the literature (*cf.* [6]). Their existence on the maximal parameter range $|\lambda| < 2$ is proved analytical in [4]. Some typically shapes of CS and CB solutions are presented in Figures 1 and 2. These solutions are of the form

$$\left(s_1(x),\ 0,\ \mathrm{sgn}(\lambda)\ \sqrt{1-s_1^2(x)}\right). \tag{13}$$

The energy of CS and CB solutions relative to the translationally invariant stationary solution (6) is shown in Figure 3. The Peierls-Nabarro barrier $E_{\mathrm{PN}} = E_{\mathrm{CB}} - E_{\mathrm{CS}}$ is shown in Figure 4.

In addition to CS and CB solutions, there does exist a one-parameter family of stationary kink solutions for a

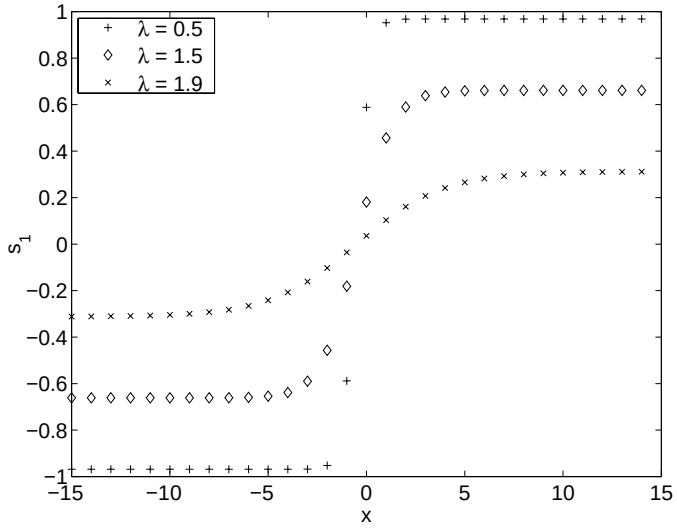

Fig. 2. CB solutions for different values of λ.

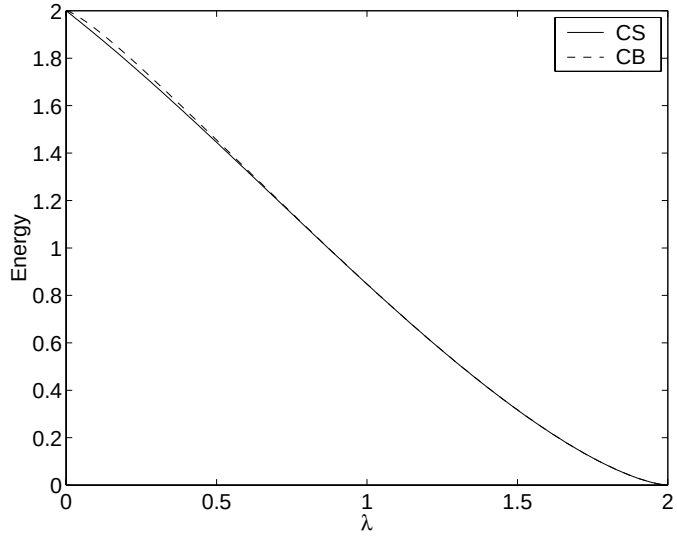

Fig. 3. Energy of the CS and CB solutions against λ.

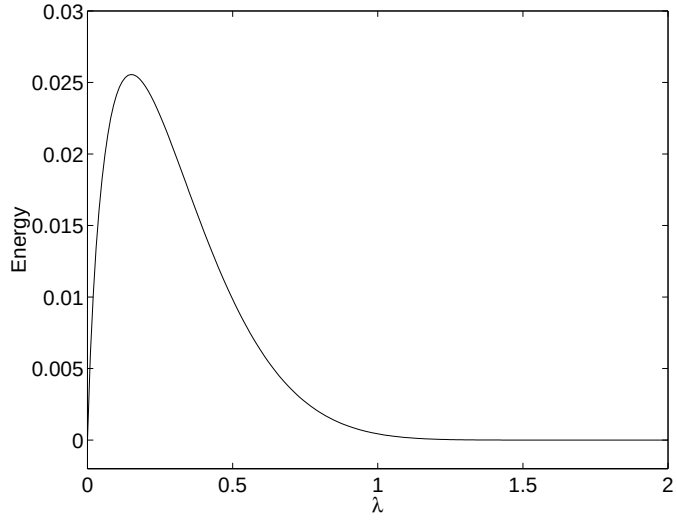

Fig. 4. Peierls-Nabarro barrier as a function of λ.

nonempty interval $|\lambda| \in]\lambda_0, 2[$. Their existence is proved analytically in [4] by use of the implicit function theorem. In general, these solutions do not admit any reflectional symmetry. They can be described by a continuous function $s_c\colon \mathbb{R} \to [-1, 1]$ and satisfy

$$(s_1(x), s_2(x), s_3(x)) = \Big(s_c(x + x_0),\ 0,\ \mathrm{sgn}(\lambda)\sqrt{1 - s_c^2(x + x_0)}\Big) \quad (14)$$

with $x \in \mathbb{Z}$ and fixed $x_0 \in \mathbb{R}$. Numerically, this family of solutions can be observed for $1.9 < |\lambda| < 2.0$. In the limit, as $|\lambda| \to 2$, it behaves as

$$\hat{s}_c(x) = \pm\sqrt{1 - \frac{\lambda^2}{4}}\ \tanh\left(\sqrt{\frac{1}{2}\left(1 - \frac{\lambda^2}{4}\right)}\ x\right). \quad (15)$$

We obtain CS solutions by choosing $x_0 \in \mathbb{Z}$. CB solutions can be obtained with $x_0 \in \mathbb{Z} + \frac{1}{2}$. The energy of this family of stationary kink solutions is independent of the shift x_0 within the range of numerical errors. Therefore, it equals E_{CS} and E_{CB}. It needs to be investigated in the future whether this numerical result can be confirmed analytically.

In [8] there has been investigated an approximative model system, obtained from equation (5) by a continuum approximation. In the limit, as $|\lambda| \to 2$, one obtains for this model system the same asymptotic behaviour as given in equation (15). It is compatible with that of the stationary kink solution given in [8] as an implicit expression only.

4 Travelling wave solutions

In the following section we consider travelling wave solutions $s_i(x, t) = s_i(x - c\ t)$ of equation (5) for a given velocity $c \in \mathbb{R}$.

4.1 Periodic solutions

First, we consider periodic solutions. In a neighbourhood of the translationally invariant stationary solutions (6) and (7) cosine shaped travelling wave solutions of small amplitude can be observed. For almost all $0 < |\lambda| < 2$ and $c \neq 0$, the existence of such solutions near the translationally invariant stationary solutions (6) has been proved analytically in [4] by use of the implicit function theorem. Their period $\frac{2\pi}{\xi}$ is given by zeroes of the characteristic equation

$$h(\xi) = 4 - c^2\xi^2 - \lambda^2\cos(\xi) = 0. \quad (16)$$

In the given parameter range, equation (16) allows at least one zero $\xi_0 > 0$. Additional zeroes appear and disappear in pairs as the parameters λ and c vary. The periodic solutions change their shape and period slightly for increasing amplitudes.

The same holds true for periodic solutions in a neighbourhood of the translationally invariant stationary solution (7). Now, the characteristic equation reads as follows

$$h(\xi) = \lambda^2 - c^2\xi^2 - 2\lambda\cos(\xi) = 0. \tag{17}$$

In the case $|\lambda| < 2$, this equation has zeroes only if $|c|$ is sufficiently small. In the case $|\lambda| > 2$, for almost all $c \neq 0$, the existence of periodic solutions can be proved analytically.

The periodic solutions investigated here are well known in the literature as *spin waves*, obtained in terms of expansions up to any order. However, for a zero set of parameter values λ and c, we run into resonances. An expansion does not even exist formally in this case.

4.2 Kink solutions

In contrast to stationary kink solutions (*i.e.*, travelling wave kink solutions with velocity $c = 0$) for kink solutions with nonzero velocity c, we allow small oscillations (*i.e.*, magnons) to be superimposed. Because of the travelling wave ansatz, these oscillations have the same velocity as the kink. Superpositions of travelling kinks and oscillations with different velocities should be investigated in the future. For nonzero velocity c, the kink looses energy while propagating through the lattice. Therefore, radiation has to be pumped into the medium to keep the kink propagating (*cf.* [1,2,7]).

The existence of kink solutions with magnons has been proved by use of the implicit function theorem for any given $|c| < \sqrt{2}$ and an open parameter range of sufficiently large $|\lambda| < 2$ (*cf.* [4]). These solutions satisfy

$$s_2(x) = \frac{c}{\lambda}\,\frac{\mathrm{d}}{\mathrm{d}x}\,s_1(x) \tag{18}$$

$$s_3(x) = \mathrm{sgn}(\lambda)\,\sqrt{1 - s_1^2(x) - s_2^2(x)}. \tag{19}$$

In the limit $|\lambda| \to 2$, the s_1-component behaves like

$$\hat{s}_1(x) = \pm\sqrt{1 - \frac{\lambda^2}{4}}\,\tanh\left(\sqrt{\frac{1}{2 - c^2}\left(1 - \frac{\lambda^2}{4}\right)}\,x\right). \tag{20}$$

In the case $\lambda = 0$, there do exist kink solutions with velocity $c = 0$ only.

In equation (20), there cannot be seen any magnons at all. Actually, the proof does not tell if there are any magnons for $|\lambda| < 2$. This is just not excluded by the proof. On the other side, it has not been possible to prove the nonexistence of magnons for $|\lambda| < 2$ and $c \neq 0$. Numerically, magnons can be observed immediately if $|\lambda|$ gets smaller than 2 (*i.e.*, the amplitude of the solution becomes larger than zero).

Figure 5 shows some typical shapes of travelling kink solutions. The corresponding asymptotic solutions (20) are plotted in addition. Figure 6 shows the range in the (λ, c)-plane where kink solutions with magnons have been observed numerically.

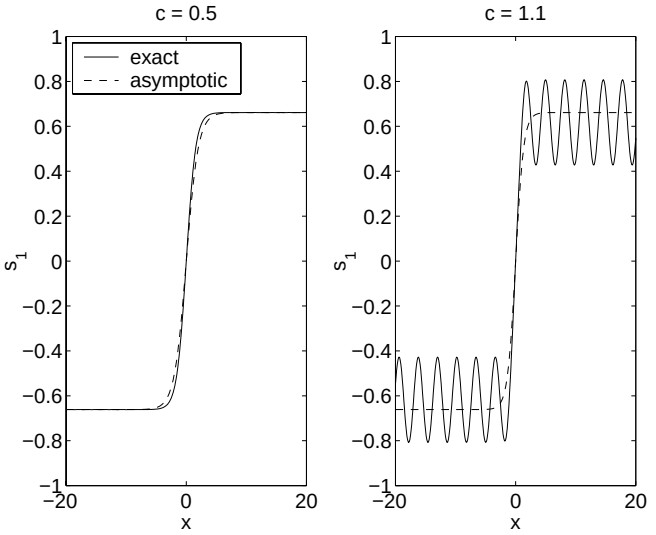

Fig. 5. Kink solutions with magnons and asymptotic solutions for $\lambda = 1.5$ and different velocities c.

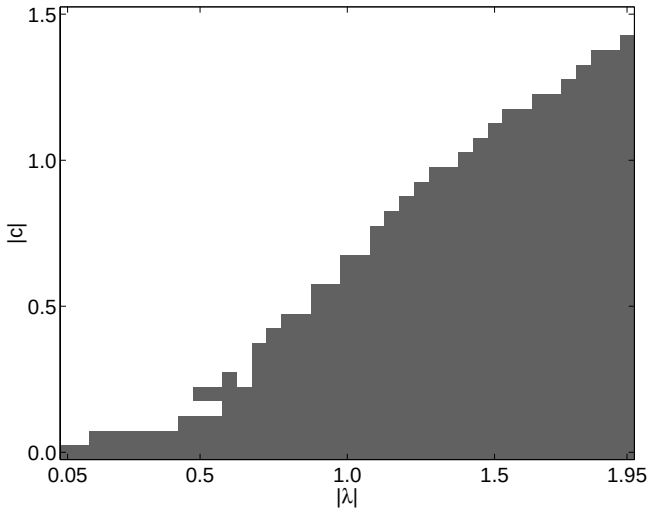

Fig. 6. Parameter range (dark) of kink solutions with magnons.

The oscillations in the tail of travelling kink solutions turn out to be described very well by the periodic solutions investigated above. In particular, the same restrictions to the period of the oscillations do apply in this case as well. Figures 7 and 8 show some typical amplitudes and periods of oscillations in numerically calculated kink solutions for $\lambda = 1.5$ and different velocities c. In addition, the corresponding periods for small-amplitude periodic solutions calculated from the characteristic equation (16) are plotted. Both periods fit very well for small amplitudes, but for increasing amplitudes they differ slightly. This effect arises, because equation (16) gives the period of *small* oscillations only. If the amplitude of the oscillation becomes larger, its period changes slightly. Both curves match exactly if one calculates the period of oscillations with the

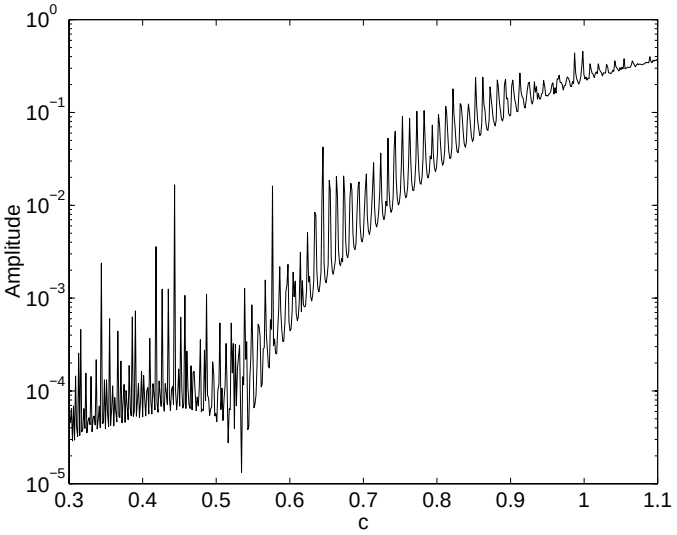

Fig. 7. Amplitude of the oscillations in the tail of travelling kink solutions for $\lambda = 1.5$.

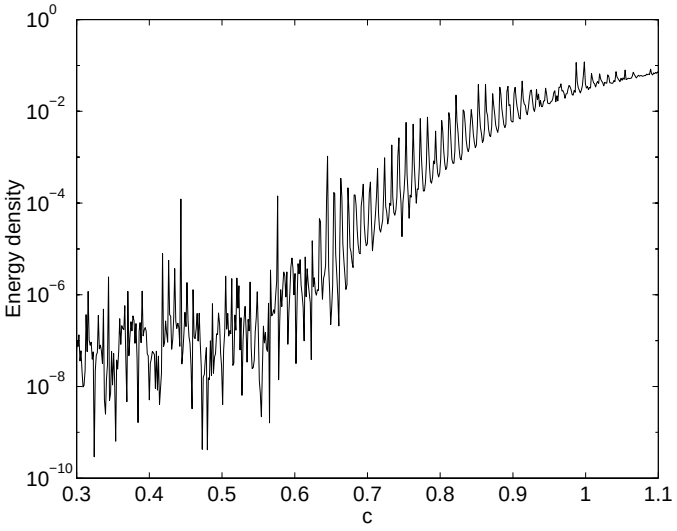

Fig. 9. Energy density of the oscillations in the tail of travelling kink solutions for $\lambda = 1.5$.

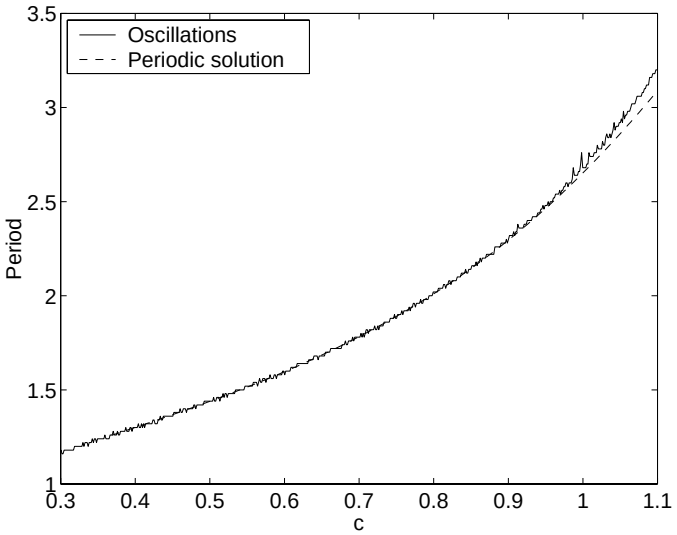

Fig. 8. Period of the oscillations in the tail of travelling kink solutions for $\lambda = 1.5$.

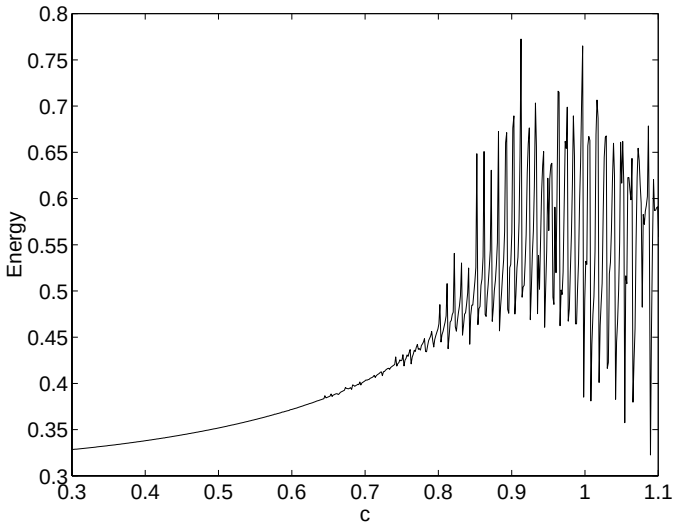

Fig. 10. Energy of the travelling kink for $\lambda = 1.5$.

same amplitude as the oscillations in the tail of the travelling kink. The small stairs in Figure 8 are caused by numerics. They represent the discretization of the real line, on which the period of the oscillations has to be measured. The spikes in Figure 7 are numerical artefacts too. They become smaller if one uses a finer grid. Actually, the period of numerically calculated oscillations tends to be a multiple of the discretization width. Now, the period depends continuously on the amplitude (and *vice versa*) and changes only slightly. Therefore, special pairs of periods and amplitudes are preferred by numerics and the amplitudes are affected most strongly by this effect.

The energy density of the oscillations in the tail of travelling kink solutions is plotted in Figure 9. The period of the oscillations varies only slowly with increasing c. Therefore, the energy density is mainly determined by their amplitude. The spikes are caused by the same numerical effect as in Figure 7. In addition, in Figure 10 there is plotted the energy of the travelling kink relative to the energy of a periodic solution with the same amplitude and period as the tail-oscillations (but without kink). For tail-oscillations of large amplitude (*i.e.*, $c > 0.8$), the kink energy is varying strongly with increasing c. Again, this effect is caused by numerics. As stated above, in the case of oscillations of large amplitude, their exact shape (*i.e.*, their amplitude) is determined by "snapping" the period to the discretization used for numerics. So, the main contribution to kink energy is due to fitting the central kink and the tail-oscillations to one another.

For the numerical calculation of travelling wave and stationary solutions, Newton's method has been used. If we plug the travelling wave ansatz $s_i(x,t) = s_i(x - c\,t)$ into equation (5), we obtain a differential difference equation

Table 1. Translationally invariant stationary solutions: Spectra and domains of stability.

Solution	Domain	Spectrum	Domain of stability
$\left(\pm\sqrt{1-\frac{\lambda^2}{4}},\ 0,\ \frac{\lambda}{2}\right)$	$\lvert\lambda\rvert < 2$	$\pm\left[\sqrt{4-\lambda^2}, \sqrt{4+\lambda^2}\right]\ i$	$\lvert\lambda\rvert < 2$
$(0,\ 0,\ \pm 1)$	$\lambda \in \mathbb{R}$	$\left\{\pm\sqrt{\lambda(2\mu-\lambda)}\ \middle\vert\ \mu \in [-1,1]\right\}$	$\lambda = 0$ or $\lvert\lambda\rvert \geq 2$
$(0,\ \cos(\mu),\ \sin(\mu))$	$\lambda = 0$	$\{0\}$	$\lambda = 0$

with both forward and backward shifted arguments. At given sites $x_j \in \mathbb{R}$, we solve the discretization of this "travelling wave equation" by Newton's method. The x_j have been chosen to be equidistant on an interval $[A, B]$ (*e.g.*, $x_j = \frac{j}{10}$ or $\frac{j}{100}$ for $c \neq 0$ and $x_j = j$ for $c = 0$). Due to the shifted arguments in the basic equation, we have to impose boundary values on two intervals $[A-1, A[$ and $]B, B+1]$. The boundary values can be chosen in accordance to the translationally invariant stationary solutions (6, 7) or (8). Much better results have been achieved by carrying out the nth Newton step on an interval $[A+n, B-n]$. Now, the boundary values on the intervals $[A+n-1, A+n[$ and $]B-n, B-n+1]$ are given by the solution of the Newton step before. The disadvantage of this method is the shrinking of the domain in every Newton step. Therefore, one has to prescribe the number of steps before starting the iteration.

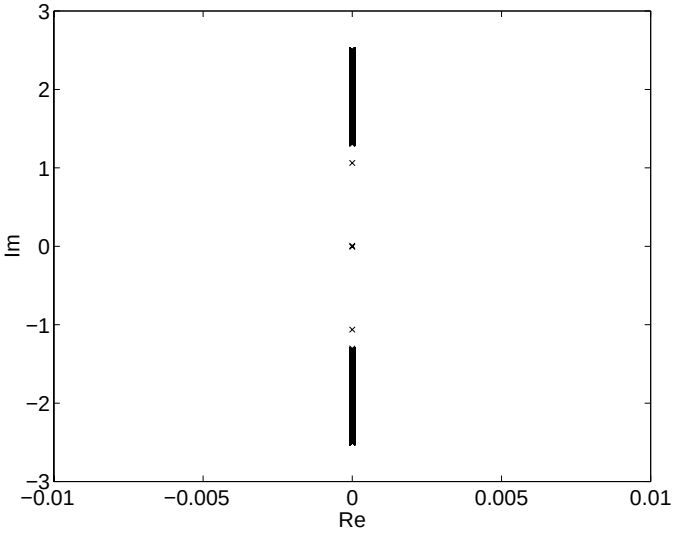

Fig. 11. Spectrum of the CS solution for $\lambda = 1.5$.

5 Spectral stability

In order to analyze stability, we linearize the equations of motion (5) around a given solution $(s_{10}(x,t), s_{20}(x,t), s_{30}(x,t))$. The perturbation ansatz

$$s_i(x,t) = s_{i0}(x,t) + s_{i1}(x,t) \tag{21}$$

gives the following set of linearized equations of motion for a perturbation $(s_{11}(x,t), s_{21}(x,t), s_{31}(x,t))$

$$\begin{aligned}
\dot{s}_{11}(x,t) &= \lambda\ s_{21}(x,t) \\
\dot{s}_{21}(x,t) &= -\lambda\ s_{11}(x,t) \\
&\quad + s_{30}(x,t)\,(s_{11}(x-1,t) + s_{11}(x+1,t)) \\
&\quad + s_{31}(x,t)\,(s_{10}(x-1,t) + s_{10}(x+1,t)) \\
\dot{s}_{31}(x,t) &= -s_{20}\,(s_{11}(x-1,t) + s_{11}(x+1,t)) \\
&\quad - s_{21}(x,t)\,(s_{10}(x-1,t) + s_{10}(x+1,t))\,.
\end{aligned} \tag{22}$$

The right hand side of equation (22) determines a linear bounded operator $F(s_{10}(t), s_{20}(t), s_{30}(t))$ mapping perturbations in $l^2(\mathbb{Z}, \mathbb{C}^3)$ to $l^2(\mathbb{Z}, \mathbb{C}^3)$. An investigation of the spectrum of the operator $F(s_{10}(t), s_{20}(t), s_{30}(t))$ will give information about the stability of the solution $(s_{10}(x,t), s_{20}(x,t), s_{30}(x,t))$. If there are contributions to the spectrum with positive real part, we will call the solution *linearly unstable*. Otherwise it will be called *spectrally stable*. Due to some freedom in choosing the angular momentum per spin $\sqrt{s_1^2(x,t) + s_2^2(x,t) + s_3^2(x,t)}$, there will be "unphysical" eigenvalues. If the solution $(s_{11}(x,t), s_{21}(x,t), s_{31}(x,t))$ is stationary, this unphysical eigenvalues will be zero. In general, they can be ruled out by requiring

$$\begin{aligned}
s_{10}(x,t)\ s_{11}(x,t) + s_{20}(x,t)\ s_{21}(x,t) \\
+ s_{30}(x,t)\ s_{31}(x,t) = 0
\end{aligned} \tag{23}$$

which is the linearization of the normalization condition $s_1^2(x,t) + s_2^2(x,t) + s_3^2(x,t) = 1$.

First, we consider the translationally invariant stationary solutions (6, 7) and (8). In this case, the operator $F(s_{10}, s_{20}, s_{30})$ is time independent. Table 1 presents the corresponding spectra and domains of stability (for an analytical proof *cf.* [4]).

Stationary kink solutions have been proved analytically to have the same essential spectra as the translationally invariant stationary solution (6) (*cf.* [4]). This holds true because, as x tends to $\pm\infty$, these solutions look like solution (6). In addition, for stationary kink solutions there does exist a nonempty discrete spectrum. These discrete spectra have to be computed numerically. Figures 11 and 12 show typical spectra of CS and CB solutions. In general, CS solutions are spectrally stable. CB solutions typically have a pair of real valued eigenvalues. Therefore, they are linearly unstable. In Figure 13, the positive real eigenvalue of the CB solution is plotted as a function of λ. For $\lambda \gtrapprox 1.9$, the real valued pair of eigenvalues becomes much smaller than numerical accuracy. This goes hand in hand with the appearance of the one-parameter family of stationary kink solutions considered in Section 3. A correlation of both phenomena has to be investigated more deeply in the future.

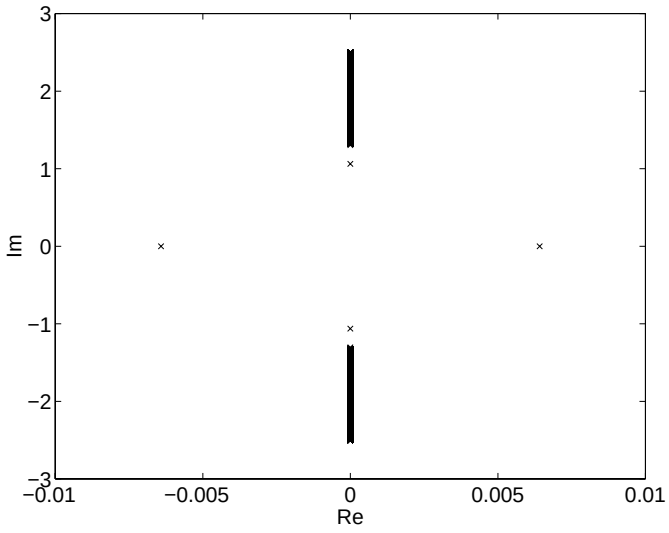

Fig. 12. Spectrum of the CB solution for $\lambda = 1.5$.

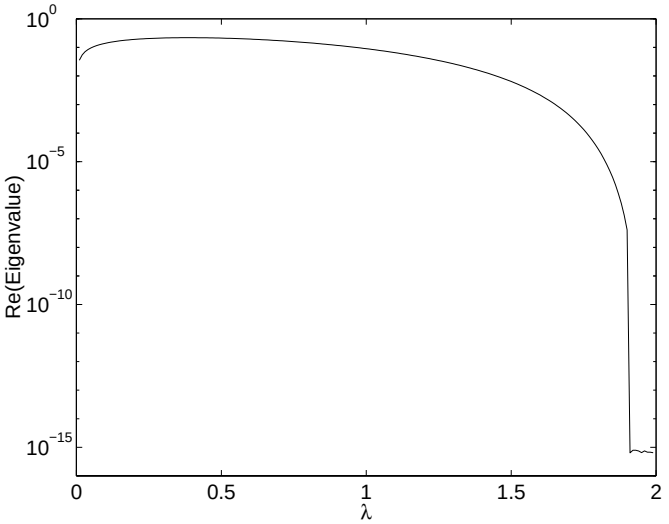

Fig. 13. Positive real eigenvalue of the CB solution against the parameter λ.

The eigenvectors, corresponding to the pair of real valued eigenvalues cause the CB solution to start travelling through the lattice. As CB solutions are linearly unstable, already a very small perturbation can cause this effect. In contrast, all eigenvalues of CS solutions are purely imaginary. Therefore, these are spectrally stable. In order to perturb a CS solution into a travelling solution, a sufficiently big amount of perturbation energy is needed. If a perturbation is too small, it will cause small oscillations around the CS solution only. This effect is called "pinning". Figures 14 and 15 show perturbations of CS and CB solutions. In the first case, pinning takes effect. In the second case, we used a suitable eigenvector for perturbation. Therefore, the kink starts travelling until it has lost enough energy by radiation to be trapped again.

For periodic travelling wave solutions and kink solutions with nonzero velocity c there are no analytical results. Numerically, they are always linearly unstable. In contradiction to the stationary solutions considered above,

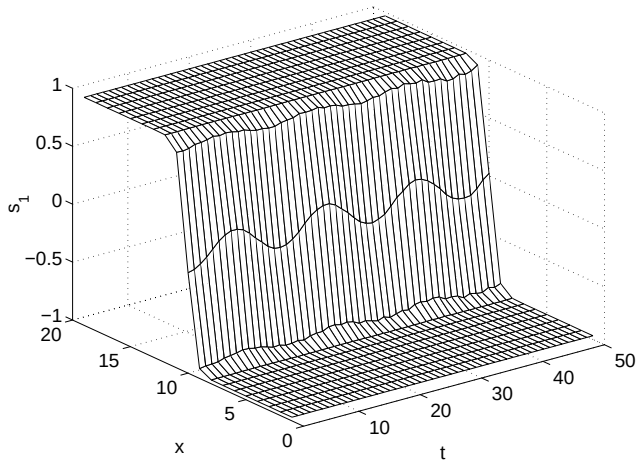

Fig. 14. Perturbation of a CS solution.

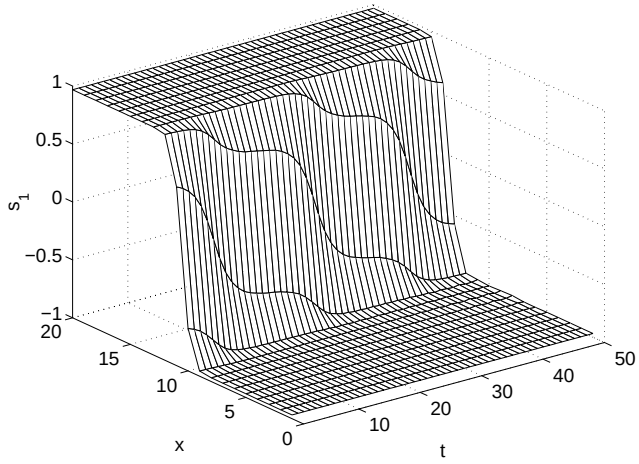

Fig. 15. Perturbation of a CB solution.

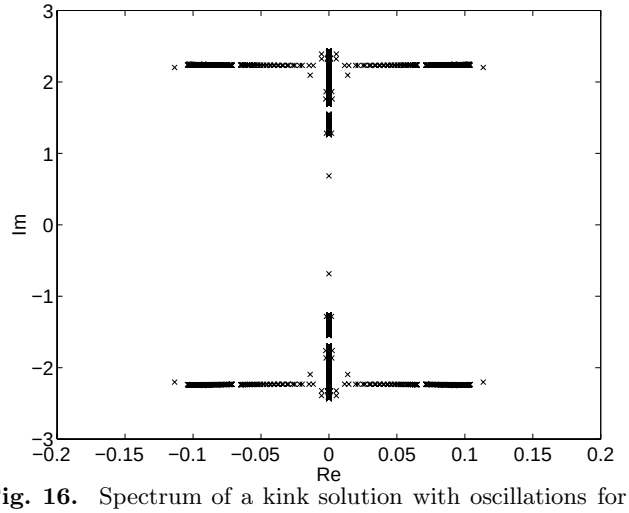

Fig. 16. Spectrum of a kink solution with oscillations for a nonzero velocity $c = 1.1$ and $\lambda = 1.5$.

there are now positive real parts in the essential spectrum. This is not surprising if the solutions vary continuously with the parameter c. Then, a slight change in shape can cause a small change in velocity. Therefore, the changed and unchanged solutions separate in time more and more. In Figure 16, a typical spectrum of a travelling wave solution with nonzero velocity c is presented.

I express my gratitude to Prof. J. Scheurle, who supervised my doctoral thesis [3] from which this paper is extracted. Proofs of the analytical results can also be found in [4].

References

1. D.B. Duncan, J.C. Eilbeck, H. Feddersen, J.A.D. Wattis, Physica D **68**, 1 (1993).
2. C. Etrich, E. Magyari, H.-J. Mikeska, H. Thomas, R. Weber, Z. Phys. B **62**, 97 (1985).
3. A. Johann, *Zur Dynamik des klassischen Ising-Modells auf dem eindimensionalen Gitter* (TU München doctoral thesis, München, 1999).
4. A. Johann, *On the dynamics of the classical transverse field Ising chain*, in J. Differential Equations (in press).
5. H.-J. Mikeska, M. Steiner, Adv. Phys. **40**, 191 (1991).
6. H.-J. Mikeska, S. Miyashita, Z. Phys. B **101**, 275 (1996).
7. M. Peyrard, M.D. Kruskal, Physica D **14**, 88 (1984).
8. P. Prelovšek, I. Sega, Phys. Lett. A **81**, 407 (1981).